JOURNAL OF MATERIALS SCIENCE 27 (1992) 5863–5868

Crystallization study of amorphous $Fe_{40}Ni_{40}B_{20}$ by electrical resistivity measurement

A. MITRA, V. RAO, S. PRAMANIK, O. N. MOHANTY
National Metallurgical Laboratory, Magnetic Materials Group, MTP division, Jamshedpur 831 007, India

The crystallization in amorphous $Fe_{40}Ni_{40}B_{20}$ alloy has been studied by electrical resistivity measurement. It shows a three stage compared to the more conventional two-stage crystallization behaviour in many metallic glasses. The Johnson–Mehl–Avrami equation was found to be operative only for 40% transformed crystallized volume for the highest measured isotherm (740 K). The Avrami exponent and activation energy were found to be 1.75 and 53 kcal mol^{-1}, respectively. The low activation energy in the amorphous alloy has been explained by the structural relaxation model.

1. Introduction

Metallic glasses based on transition metals are soft magnetic materials and are extensively used in the electronic and power industries [1]. The metastable nature of the different phases, however, makes them unsuitable for use in the industry in its as-quenched state. Consequently, the manner in which these phases proceed towards equilibrium is not only of fundamental interest but of technical importance as well.

Amongst the transition metal-based metallic glasses, Fe–Ni–M (where M is the metalloid) materials are the most extensively studied system because of their interesting magnetic properties coupled with high strength and good corrosion resistance [2–4]. $Fe_{40}Ni_{40}B_{20}$ is a simple ternary system whose thermal behaviour has been reported by several researchers employing techniques such as calorimetry, dilatometry, magnetometry, resistometry [5–9]. Differential scanning calorimetry (DSC), however, is used widely for studying crystallization behaviour.

In the present work the thermal behaviour of amorphous $Fe_{40}Ni_{40}B_{20}$ alloy has been studied using electrical resistivity measurements. The crystallization and Curie temperatures have also been determined by DSC and magnetization studies.

2. Experimental procedure

The metallic glass studied here, prepared by the melt spinning technique, had a nominal composition $Fe_{40}Ni_{40}B_{20}$. The electrical resistivity measurements were made by a d.c. four-probe method using an infrared gold image furnace (TER-2000, Ulvac/Sinku-Rico, Japan) where the temperature could be varied from 300–1400 K. A 1 mA current was passed through the sample during the measurement. Typical dimensions of the sample were 3 cm × 0.2 cm × 30 μm. During isothermal measurements, the sample was kept at the desired temperature for sufficient time for the resistivity to become constant. The calorimetric study was carried out using a Perkin-Elmer DSC-7 calorimeter. Magnetization was measured using a vibrating sample magnetometer at a residual magnetic field strength of 3.5 kA m^{-1}. The X-ray diffractograms of the alloys heat-treated at different temperatures for 30 min were taken using a Siemens-D500 diffractometer using Cr K_α radiation. The microstructure of the sample annealed at 630 K for 20 min was studied by electron microscopy (Philips EM-400). A circular specimen, 3 mm diameter, was punched out and electrolytically thinned and polished in a mixture of 90% acetic acid and 10% percholoric acid using a twin-jet Struers tenupole – 2.

3. Results and discussion

The temperature variation of normalized resistivity (ρ_T/ρ_{290}) measured at a heating rate of 5 K min^{-1}, is shown in Fig. 1. The resistivity increases with temperature up to 470 K with the temperature coefficient of resistivity (TCR $= (1/\rho_{290})(d\rho/dT)$) 1.934×10^{-4} K^{-1}. From 470 K onwards, the value of TCR begins to change. A small decrease in resistivity is observed at 600 K which is shown much more prominently in Fig. 1b. Resistivity drops sharply at 730 K showing the onset of primary crystallization. Another drop in resistivity is observed at 870 K which corresponds to the crystallization of secondary phases. The DSC study of the same sample showed similar different transitions (Fig. 2). Two sharp exothermic peaks at 766 K and 845 K and a broad exothermic maximum in the temperature range 500–660 K were observed. This broad maximum may be attributed to the superposition of two transitions which are observed at 470 and 600 K in the resistivity measurement. $Fe_{40}Ni_{40}B_{20}$ is a ferromagnetic material at room temperature. The Curie temperature of this alloy is

0022–2461

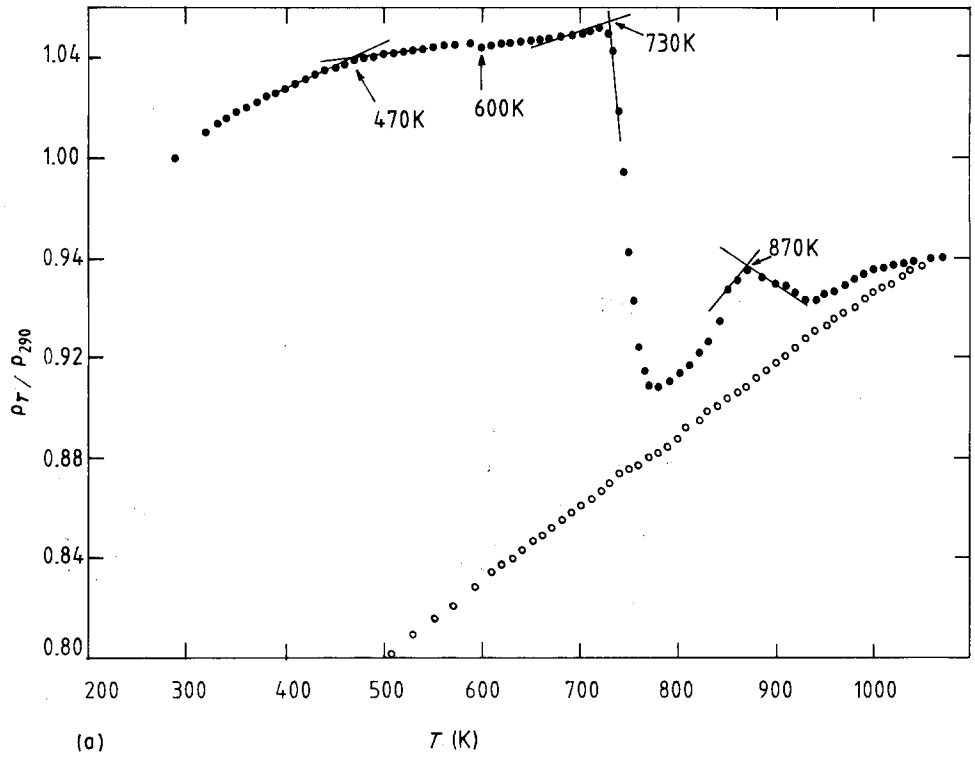

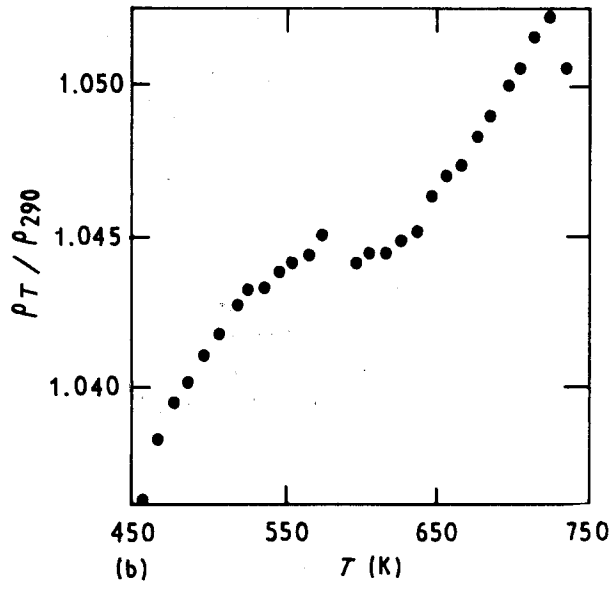

Figure 1 (a, b) Plot of normalized resistivity, ρ_T/ρ_{290}, versus temperature for $Fe_{40}Ni_{40}B_{20}$ showing different transitions. The heating (●) and cooling (○) rate is 5 K min^{-1}.

478 K, as determined from magnetization measurement (Fig. 3). Hence, the transition which is observed at 470 K in the resistivity measurements is related to the ferro to paramagnetic transition. The other three transitions at 600, 730 and 870 K observed from the resistivity measurements are related to the crystallization of $Fe_{40}Ni_{40}B_{20}$ alloy. These three stages of crystallization are unusual and so far only a two-stage crystallization behaviour has been reported for the amorphous alloys [10] where the primary crystallization is related to the crystallization of transition metal-rich phases, and other crystallization involves the crystallization of the metalloid-enriched phases through the eutectoid reaction. The cause of the new transition which is observed at 600 K during the resistivity measurements is not completely known. This transition may be attributed to the atomic rearrangement during the relaxation of internal stress produced during preparation, or due to the formation of small crystalline particles. To obtain some idea of the different crystallized phases, X-ray diffractograms were taken for the samples annealed for 30 min at different temperatures close to different transition points. Fig. 4 shows the diffractograms for samples annealed for 30 min at 630, 730, 920 and 1070 K. It is revealed that the transition which occurs at 730 K in the resistivity (or 766 K in DSC) measurements corresponds to the crystallization of γ-(FeNi) phase. The transition corresponds to 870 K in the resistivity (or 845 K in DSC) measurements and is related to the crystallization of $(FeNi)_3B$ and $Fe_{4.5}Ni_{18.5}B_6$ phases. These phases observed after crystallization are in agreement with previously reported results [11]. An X-ray diffractogram of the sample annealed at 630 K shows a broad maximum in the region where the most intense peaks of the crystallized sample appear. This broad maximum is neither characteristic of amorphous alloy nor of the crystalline state. The microstructure of the sample annealed at 630 K for 20 min was studied by TEM: small grains, of the order of 100 nm in size, were seen (Fig. 5). Fig. 5b shows the selected-area diffraction pattern, the diffused diffraction rings indicating the existence of small crystalline particles in the system. Therefore, it can be concluded from X-ray and TEM studies that the transition at 600 K in the resistivity measurements is probably due to the formation of small crystallites of transition metal-based phases which are fully crystallized at higher temperatures.

The crystallization kinetics of γ-(FeNi) phase have also been studied from the resistivity measurements.

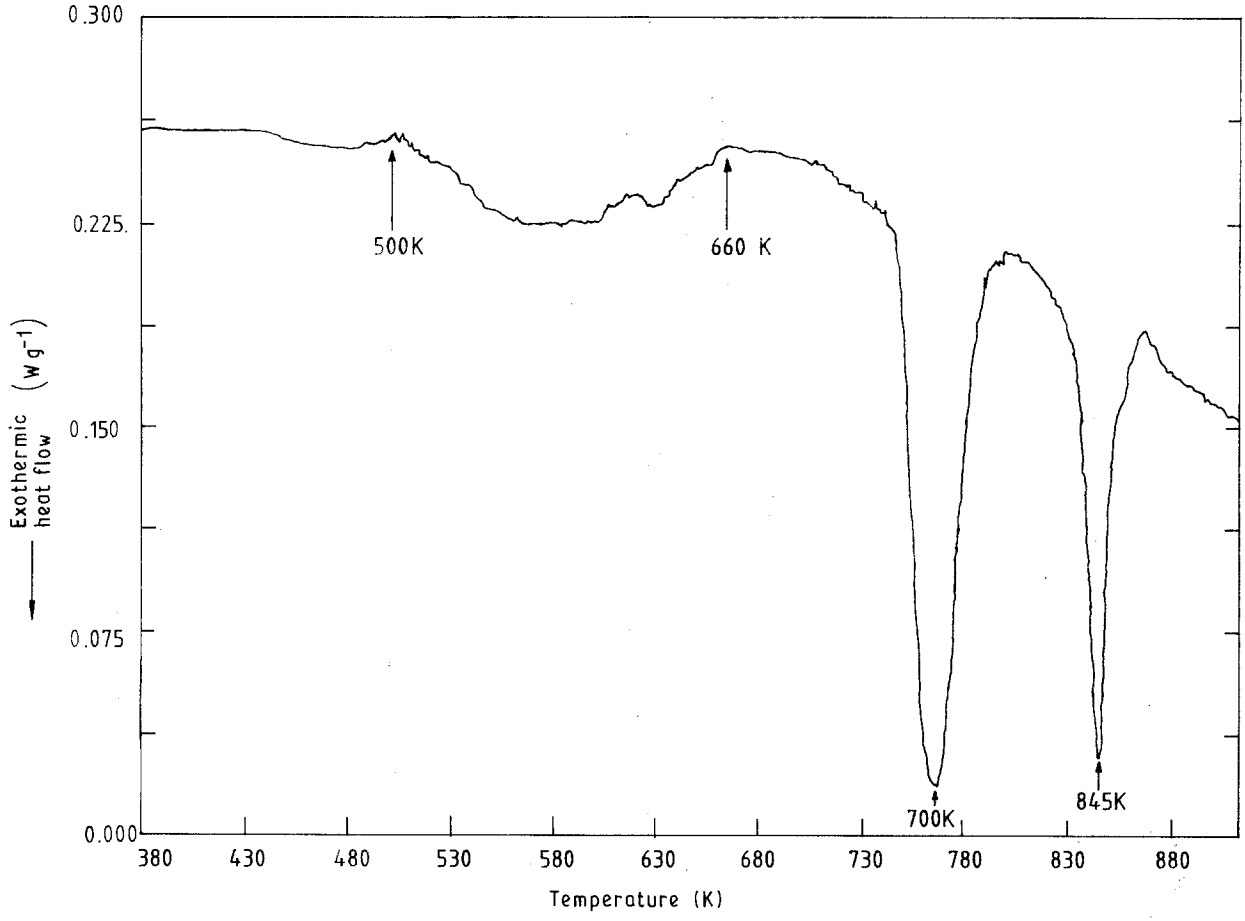

Figure 2 DSC curve of $Fe_{40}Ni_{40}B_{20}$ taken at a heating rate of 5 K min^{-1}.

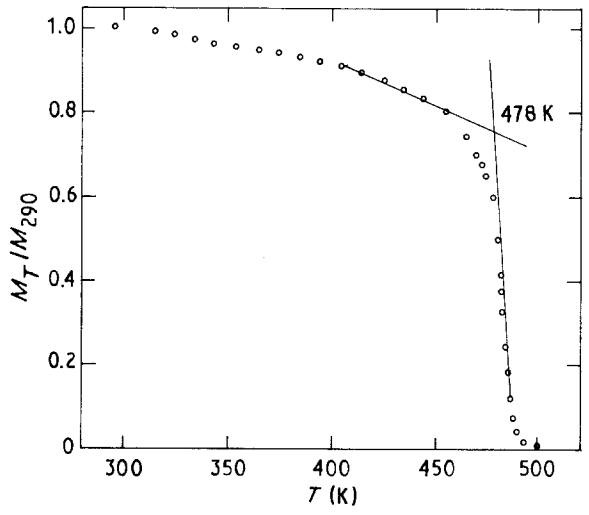

Figure 3 Variation of normalized magnetization, M_T/M_{290}, with temperature, T, to determine the ferromagnetic Curie temperature.

The crystallized volume fraction, X_t, at a time, t, during isothermal heating is determined from

$$X_t = \frac{\rho_0 - \rho_t}{\rho_0 - \rho_\alpha} \quad (1)$$

where ρ_0 and ρ_t are, respectively, the resistivity at $t = 0$ and at a time, t, after the attainment of the desired temperature. ρ_α is the constant value of the resistivity after holding the sample at that temperature for a sufficiently long time. The volume fraction transformed at three different isothermal heating temperatures (700, 720, 740 K) is plotted in Fig. 6. The kinetics of the transformation have been analysed in terms of the well-known Johnson–Mehl–Avrami equation [12]

$$X_t = 1 - \exp(-bt^n) \quad (2)$$

which can be rearranged as

$$\log[-\log(1 - X_t)] = \log(b/2.303) + n\log t \quad (3)$$

where b is a rate constant and n is the Avrami exponent. Different n values give different types of nucleation and growth mechanisms of the transformed region; for example, $n = 4$ gives a constant nucleation rate with three-dimensional growth, $n = 3$ gives three-dimensional growth with zero nucleation rate, and $n = 2$ corresponds to two-dimensional growth of disc-shaped quenched-in nuclei with zero nucleation rate [13]. The Avrami exponent was obtained by plotting $\log[-\log(1 - X_t)]$ against $\log(t - t_0)$ as shown in Fig. 7 where t_0 is the incubation period. Approximately parallel straight lines with slope $n = 1.75$ were obtained for $X_t < 40\%$ indicating that two-dimensional growth takes place during crystallization of γ-(FeNi) phase. The deviation from

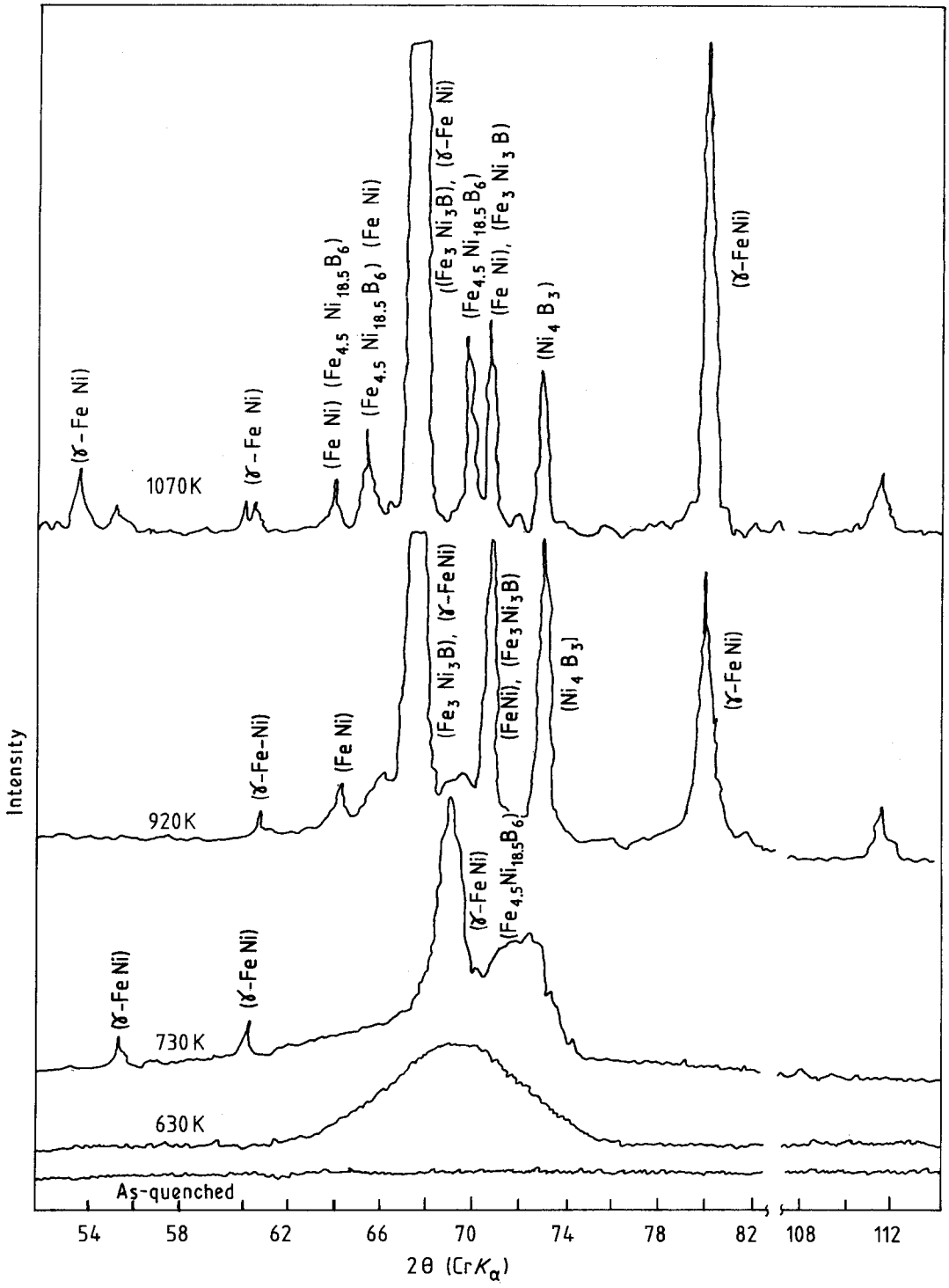

Figure 4 X-ray diffractograms of samples annealed at different temperatures for 30 min.

linearity for higher isotherms is probably due to the grain growth of the crystallites already present becoming significant, and a different mechanism is probably operative. The activation energy for the primary crystallization corresponding to only 25% transformation of the volume to crystallization is estimated using an Arrhenius type of equation

$$t_{0.25} = A\exp(-E_a/kT) \quad (4)$$

where A is a constant, k is the Boltzmann constant and E_a is the activation energy. The plot $t_{0.25}$ against $1/T$ shows a straight line which gives an activation energy of 53 kcal mol^{-1} (Fig. 8). This is of the same order as determined by other methods (77 kcal mol^{-1}) [11]. The observed values of the activation energies of metallic glasses can be explained by the structural relaxation model, where the crystallization process is assumed to occur by a coordinated motion of all atomic species rather than the diffusion of a single species [14]. For this reason, it is very difficult to obtain a controlled amount of crystallization in amorphous alloys. Calculation based on the above model shows that the activation energy ranges from 20 kcal mol^{-1} for unstable glasses to 100 kcal mol^{-1} or more for stable glasses. The measured activation

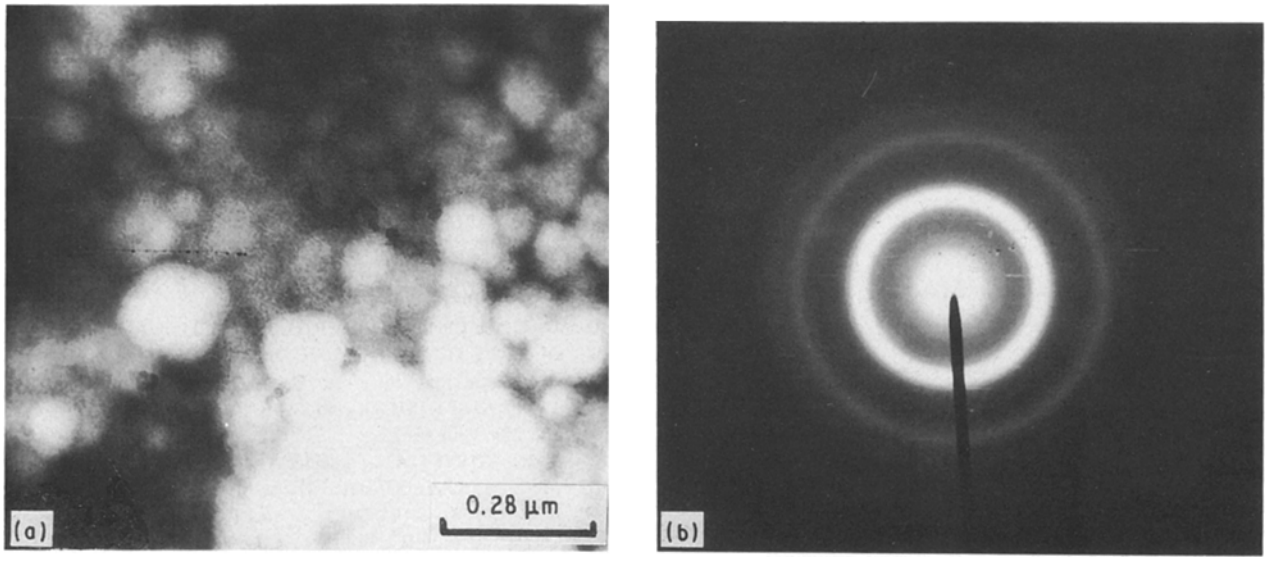

Figure 5 (a) Transmission electron micrograph of the sample annealed at 630 K for 20 min. (b) Selected-area diffraction pattern of the same region.

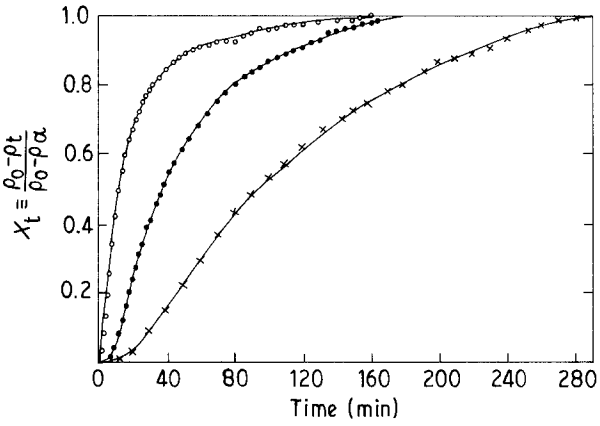

Figure 6 Plot of volume fraction transformed with time at (×) 700 K, (●) 720 K and (○) 740 K.

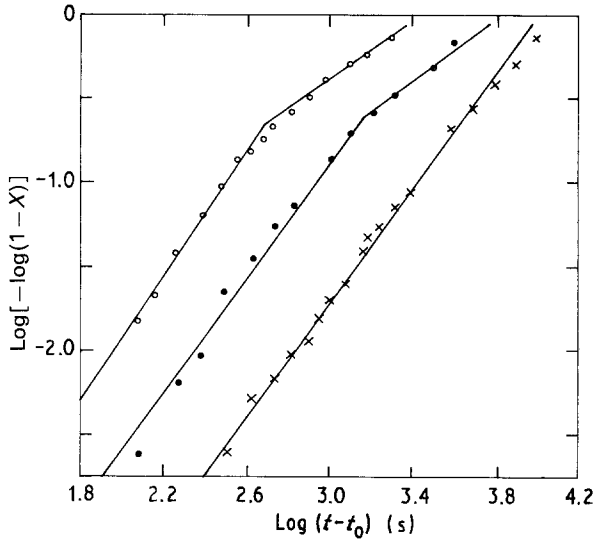

Figure 7 Johnson–Mehl–Avrami plot.

energy of $Fe_{40}Ni_{40}B_{20}$ alloy indicates that the crystallization occurs by the co-ordinated motion of different atom species.

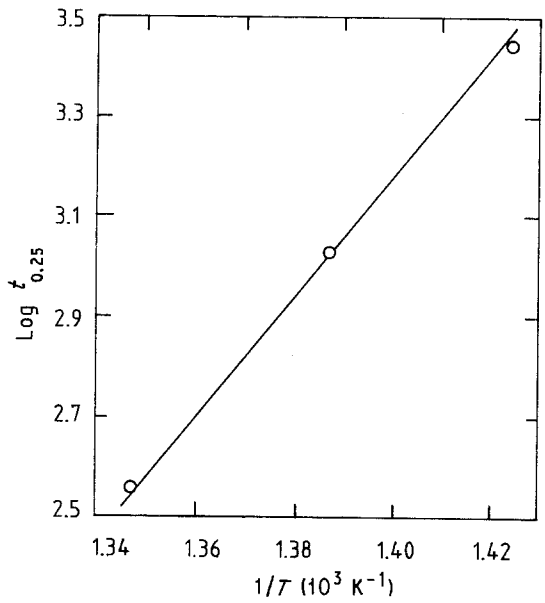

Figure 8 Plot of the time for 25% transformation of crystallized volume at different isotherms, against $1/T$. $E_a = 53$ kcal mol^{-1}.

4. Conclusion

The electrical resistivity measurement coupled with the DSC studies have shown that the $Fe_{40}Ni_{40}B_{20}$ alloy crystallizes in three different stages. Resistivity and DSC measurement together with an X-ray study show that the transition at 600 K is due to the formation of small crystallites of γ-(FeNi) phase. Primary crystallization involving the crystallization of γ-(FeNi) phase occurs around 730 K. Crystallization of the metalloid-rich phases, namely $(FeNi)_3B$ and $Fe_{4.5}Ni_{18.5}B_6$, takes place at about 840–870 K. The crystallization kinetics of primary crystallization (crystallization of γ-(Fe–Ni) phase) is well fitted by the Johnson–Mehl–Avrami equation for $X < 40\%$ with an Avrami exponent $n = 1.75$, and an activation energy $E_a = 53$ kcal mol^{-1}. These results are of the same order as those obtained from the DSC

measurement by other researchers ($n = 2.02$ and $E_a = 77\,\text{kcal mol}^{-1}$) [11]. The low value of the activation energy observed in the present study, as is usually observed for most of the metallic glasses, can be explained by the structural relaxation model.

Acknowledgement

The authors thank Professor K. P. Gupta, Indian Institute of Technology, Kanpur, for the magnetic measurements.

References

1. F. E. LUBORSKY and L. A. JOHNSON, *J. Phys.* **C8** (1980) 820. G. E. Fish, *IEEE Trans.* **Mag-78** (1990) 947.
2. L. DAVIS, in "Proceedings of the 2nd International Conference on Rapidly Quenched Metals", Vol. I (MIT Press, Boston, 1976) p. 369.
3. P. J. FLANDER, C. D. GRAHAM and T. EGAMI, *IEEE Trans.* **Mag-11** (1975) 1323.
4. D. LEE and T. M. DEVINE, in "Proceedings of the International Conference on Rapidly Quenched Metals", Vol. I (MIT
5. M. G. SCOTT, *J. Mater. Sci.* **13** (1978) 291.
6. A. KURSUMOVIC, E. GIRT, E. BABIC, M. G. SCOTT and H. H. LIEBERMANN, in "Phase Transition in Crystalline and Amorphous Alloy", edited by B. L. Mordike (Deutsche Gesellschaft fur Metallkunde, Oberursel, Germany, 1983) p. 75.
7. H. R. SINNING, G. CIZERON and R. W. CAHN, *ibid.*, p. 183.
8. G. E. FISH and R. HASEGAWA, *J. Appl. Phys.* **63** (1988) 2986.
9. A. ROIG, J. S. MUNOZ, M. B. SALAMON and K. V. RAO, *ibid.* **61** (1987) 3647.
10. U. KOSTER and U. HEROLD, in "Glassy Metals", Vol. I, edited by H. J. Guntherodt and H. Beck (Springer Verlag, Berlin, 1981) p. 225.
11. V. S. RAJA, KISHORE and S. RANGANATHAN, *J. Mater. Sci.* **25** (1990) 4667.
12. J. W. CHRISTIAN, in "The Theory of Transformation in Metals and Alloys", Part I (Pergamon Press, Oxford, 1975).
13. K. RUSSEW, S. BUDUROV and L. ANSTIEV, in 'Rapidly Quenched Metals", Vol. I, edited by S. Steeb and H. Warlimont (Elsevier Science, New York 1985) p. 283.
14. E. COLEMAN, *Mater. Sci. Engng* **23** (1976) 161.

Received 2 September 1991
and accepted 16 January 1992